Isolated Photon Cross Section in $p\bar{p}$ Collisions at $\sqrt{s} = 1.8$ TeV

B. Abbott,[47] M. Abolins,[44] V. Abramov,[19] B. S. Acharya,[13] D. L. Adams,[54] M. Adams,[30] S. Ahn,[29] V. Akimov,[17] G. A. Alves,[2] N. Amos,[43] E. W. Anderson,[36] M. M. Baarmand,[49] V. V. Babintsev,[19] L. Babukhadia,[49] A. Baden,[40] B. Baldin,[29] S. Banerjee,[13] J. Bantly,[53] E. Barberis,[22] P. Baringer,[37] J. F. Bartlett,[29] U. Bassler,[9] A. Belyaev,[18] S. B. Beri,[11] G. Bernardi,[9] I. Bertram,[20] V. A. Bezzubov,[19] P. C. Bhat,[29] V. Bhatnagar,[11] M. Bhattacharjee,[49] G. Blazey,[31] S. Blessing,[27] A. Boehnlein,[29] N. I. Bojko,[19] F. Borcherding,[29] A. Brandt,[54] R. Breedon,[23] G. Briskin,[53] R. Brock,[44] G. Brooijmans,[29] A. Bross,[29] D. Buchholz,[32] V. Buescher,[48] V. S. Burtovoi,[19] J. M. Butler,[41] W. Carvalho,[3] D. Casey,[44] Z. Casilum,[49] H. Castilla-Valdez,[15] D. Chakraborty,[49] K. M. Chan,[48] S. V. Chekulaev,[19] W. Chen,[49] D. K. Cho,[48] S. Choi,[26] S. Chopra,[27] B. C. Choudhary,[26] J. H. Christenson,[29] M. Chung,[30] D. Claes,[45] A. R. Clark,[22] W. G. Cobau,[40] J. Cochran,[26] L. Coney,[34] B. Connolly,[27] W. E. Cooper,[29] D. Coppage,[37] D. Cullen-Vidal,[53] M. A. C. Cummings,[31] D. Cutts,[53] O. I. Dahl,[22] K. Davis,[21] K. De,[54] K. Del Signore,[43] M. Demarteau,[29] D. Denisov,[29] S. P. Denisov,[19] H. T. Diehl,[29] M. Diesburg,[29] G. Di Loreto,[44] P. Draper,[54] Y. Ducros,[10] L. V. Dudko,[18] S. R. Dugad,[13] A. Dyshkant,[19] D. Edmunds,[44] J. Ellison,[26] V. D. Elvira,[49] R. Engelmann,[49] S. Eno,[40] G. Eppley,[56] P. Ermolov,[18] O. V. Eroshin,[19] J. Estrada,[48] H. Evans,[46] V. N. Evdokimov,[19] T. Fahland,[25] S. Feher,[29] D. Fein,[21] T. Ferbel,[48] H. E. Fisk,[29] Y. Fisyak,[50] E. Flattum,[29] F. Fleuret,[22] M. Fortner,[31] K. C. Frame,[44] S. Fuess,[29] E. Gallas,[29] A. N. Galyaev,[19] P. Gartung,[26] V. Gavrilov,[17] R. J. Genik II,[20] K. Genser,[29] C. E. Gerber,[29] Y. Gershtein,[53] B. Gibbard,[50] R. Gilmartin,[27] G. Ginther,[48] B. Gobbi,[32] B. Gómez,[5] G. Gómez,[40] P. I. Goncharov,[19] J. L. González Solís,[15] H. Gordon,[50] L. T. Goss,[55] K. Gounder,[26] A. Goussiou,[49] N. Graf,[50] P. D. Grannis,[49] D. R. Green,[29] J. A. Green,[36] H. Greenlee,[29] S. Grinstein,[1] P. Grudberg,[22] S. Grünendahl,[29] G. Guglielmo,[52] A. Gupta,[13] S. N. Gurzhiev,[19] G. Gutierrez,[29] P. Gutierrez,[52] N. J. Hadley,[40] H. Haggerty,[29] S. Hagopian,[27] V. Hagopian,[27] K. S. Hahn,[48] R. E. Hall,[24] P. Hanlet,[42] S. Hansen,[29] J. M. Hauptman,[36] C. Hays,[46] C. Hebert,[37] D. Hedin,[31] A. P. Heinson,[26] U. Heintz,[41] T. Heuring,[27] R. Hirosky,[30] J. D. Hobbs,[49] B. Hoeneisen,[6] J. S. Hoftun,[53] F. Hsieh,[43] A. S. Ito,[29] S. A. Jerger,[44] R. Jesik,[33] T. Joffe-Minor,[32] K. Johns,[21] M. Johnson,[29] A. Jonckheere,[29] M. Jones,[28] H. Jöstlein,[29] S. Y. Jun,[32] S. Kahn,[50] E. Kajfasz,[8] D. Karmanov,[18] D. Karmgard,[34] R. Kehoe,[34] S. K. Kim,[14] B. Klima,[29] C. Klopfenstein,[23] B. Knuteson,[22] W. Ko,[23] J. M. Kohli,[11] D. Koltick,[35] A. V. Kostritskiy,[19] J. Kotcher,[50] A. V. Kotwal,[46] A. V. Kozelov,[19] E. A. Kozlovsky,[19] J. Krane,[36] M. R. Krishnaswamy,[13] S. Krzywdzinski,[29] M. Kubantsev,[38] S. Kuleshov,[17] Y. Kulik,[49] S. Kunori,[40] G. Landsberg,[53] A. Leflat,[18] F. Lehner,[29] J. Li,[54] Q. Z. Li,[29] J. G. R. Lima,[3] D. Lincoln,[29] S. L. Linn,[27] J. Linnemann,[44] R. Lipton,[29] J. G. Lu,[4] A. Lucotte,[49] L. Lueking,[29] C. Lundstedt,[45] A. K. A. Maciel,[31] R. J. Madaras,[22] V. Manankov,[18] S. Mani,[23] H. S. Mao,[4] R. Markeloff,[31] T. Marshall,[33] M. I. Martin,[29] R. D. Martin,[30] K. M. Mauritz,[36] B. May,[32] A. A. Mayorov,[33] R. McCarthy,[49] J. McDonald,[27] T. McKibben,[30] T. McMahon,[51] H. L. Melanson,[29] M. Merkin,[18] K. W. Merritt,[29] C. Miao,[53] H. Miettinen,[56] A. Mincer,[47] C. S. Mishra,[29] N. Mokhov,[29] N. K. Mondal,[13] H. E. Montgomery,[29] M. Mostafa,[1] H. da Motta,[2] E. Nagy,[8] F. Nang,[21] M. Narain,[41] V. S. Narasimham,[13] H. A. Neal,[43] J. P. Negret,[5] S. Negroni,[8] D. Norman,[55] L. Oesch,[43] V. Oguri,[3] B. Olivier,[9] N. Oshima,[29] D. Owen,[44] P. Padley,[56] A. Para,[29] N. Parashar,[42] R. Partridge,[53] N. Parua,[7] M. Paterno,[48] A. Patwa,[49] B. Pawlik,[16] J. Perkins,[54] M. Peters,[28] R. Piegaia,[1] H. Piekarz,[27] Y. Pischalnikov,[35] B. G. Pope,[44] E. Popkov,[34] H. B. Prosper,[27] S. Protopopescu,[50] J. Qian,[43] P. Z. Quintas,[29] R. Raja,[29] S. Rajagopalan,[50] N. W. Reay,[38] S. Reucroft,[42] M. Rijssenbeek,[49] T. Rockwell,[44] M. Roco,[29] P. Rubinov,[32] R. Ruchti,[34] J. Rutherfoord,[21] A. Santoro,[2] L. Sawyer,[39] R. D. Schamberger,[49] H. Schellman,[32] A. Schwartzman,[1] J. Sculli,[47] N. Sen,[56] E. Shabalina,[18] H. C. Shankar,[13] R. K. Shivpuri,[12] D. Shpakov,[49] M. Shupe,[21] R. A. Sidwell,[38] H. Singh,[26] J. B. Singh,[11] V. Sirotenko,[31] P. Slattery,[48] E. Smith,[52] R. P. Smith,[29] R. Snihur,[32] G. R. Snow,[45] J. Snow,[51] S. Snyder,[50] J. Solomon,[30] X. F. Song,[4] V. Sorín,[1] M. Sosebee,[54] N. Sotnikova,[18] M. Souza,[2] N. R. Stanton,[38] G. Steinbrück,[46] R. W. Stephens,[54] M. L. Stevenson,[22] F. Stichelbaut,[50] D. Stoker,[25] V. Stolin,[17] D. A. Stoyanova,[19] M. Strauss,[52] K. Streets,[47] M. Strovink,[22] L. Stutte,[29] A. Sznajder,[3] J. Tarazi,[25] M. Tartaglia,[29] T. L. T. Thomas,[32] J. Thompson,[40] D. Toback,[40] T. G. Trippe,[22] A. S. Turcot,[43] P. M. Tuts,[46] P. van Gemmeren,[29] V. Vaniev,[19] N. Varelas,[30] A. A. Volkov,[19] A. P. Vorobiev,[19] H. D. Wahl,[27] J. Warchol,[34] G. Watts,[57] M. Wayne,[34] H. Weerts,[44] A. White,[54] J. T. White,[55] J. A. Wightman,[36] S. Willis,[31] S. J. Wimpenny,[26] J. V. D. Wirjawan,[55] J. Womersley,[29] D. R. Wood,[42] R. Yamada,[29] P. Yamin,[50] T. Yasuda,[29] K. Yip,[29] S. Youssef,[27] J. Yu,[29] Y. Yu,[14] M. Zanabria,[5] H. Zheng,[34] Z. Zhou,[36] Z. H. Zhu,[48] M. Zielinski,[48] D. Zieminska,[33] A. Zieminski,[33] V. Zutshi,[48] E. G. Zverev,[18] and A. Zylberstejn[10]

(D0 Collaboration)

 0031-9007/00/84(13)/2786(6)$15.00

[1]*Universidad de Buenos Aires, Buenos Aires, Argentina*
[2]*LAFEX, Centro Brasileiro de Pesquisas Físicas, Rio de Janeiro, Brazil*
[3]*Universidade do Estado do Rio de Janeiro, Rio de Janeiro, Brazil*
[4]*Institute of High Energy Physics, Beijing, People's Republic of China*
[5]*Universidad de los Andes, Bogotá, Colombia*
[6]*Universidad San Francisco de Quito, Quito, Ecuador*
[7]*Institut des Sciences Nucléaires, IN2P3-CNRS, Universite de Grenoble 1, Grenoble, France*
[8]*Centre de Physique des Particules de Marseille, IN2P3-CNRS, Marseille, France*
[9]*LPNHE, Universités Paris VI and VII, IN2P3-CNRS, Paris, France*
[10]*DAPNIA/Service de Physique des Particules, CEA, Saclay, France*
[11]*Panjab University, Chandigarh, India*
[12]*Delhi University, Delhi, India*
[13]*Tata Institute of Fundamental Research, Mumbai, India*
[14]*Seoul National University, Seoul, Korea*
[15]*CINVESTAV, Mexico City, Mexico*
[16]*Institute of Nuclear Physics, Kraków, Poland*
[17]*Institute for Theoretical and Experimental Physics, Moscow, Russia*
[18]*Moscow State University, Moscow, Russia*
[19]*Institute for High Energy Physics, Protvino, Russia*
[20]*Lancaster University, Lancaster, United Kingdom*
[21]*University of Arizona, Tucson, Arizona 85721*
[22]*Lawrence Berkeley National Laboratory and University of California, Berkeley, California 94720*
[23]*University of California, Davis, California 95616*
[24]*California State University, Fresno, California 93740*
[25]*University of California, Irvine, California 92697*
[26]*University of California, Riverside, California 92521*
[27]*Florida State University, Tallahassee, Florida 32306*
[28]*University of Hawaii, Honolulu, Hawaii 96822*
[29]*Fermi National Accelerator Laboratory, Batavia, Illinois 60510*
[30]*University of Illinois at Chicago, Chicago, Illinois 60607*
[31]*Northern Illinois University, DeKalb, Illinois 60115*
[32]*Northwestern University, Evanston, Illinois 60208*
[33]*Indiana University, Bloomington, Indiana 47405*
[34]*University of Notre Dame, Notre Dame, Indiana 46556*
[35]*Purdue University, West Lafayette, Indiana 47907*
[36]*Iowa State University, Ames, Iowa 50011*
[37]*University of Kansas, Lawrence, Kansas 66045*
[38]*Kansas State University, Manhattan, Kansas 66506*
[39]*Louisiana Tech University, Ruston, Louisiana 71272*
[40]*University of Maryland, College Park, Maryland 20742*
[41]*Boston University, Boston, Massachusetts 02215*
[42]*Northeastern University, Boston, Massachusetts 02115*
[43]*University of Michigan, Ann Arbor, Michigan 48109*
[44]*Michigan State University, East Lansing, Michigan 48824*
[45]*University of Nebraska, Lincoln, Nebraska 68588*
[46]*Columbia University, New York, New York 10027*
[47]*New York University, New York, New York 10003*
[48]*University of Rochester, Rochester, New York 14627*
[49]*State University of New York, Stony Brook, New York 11794*
[50]*Brookhaven National Laboratory, Upton, New York 11973*
[51]*Langston University, Langston, Oklahoma 73050*
[52]*University of Oklahoma, Norman, Oklahoma 73019*
[53]*Brown University, Providence, Rhode Island 02912*
[54]*University of Texas, Arlington, Texas 76019*
[55]*Texas A&M University, College Station, Texas 77843*
[56]*Rice University, Houston, Texas 77005*
[57]*University of Washington, Seattle, Washington 98195*

(Received 10 December 1999)

We report a new measurement of the cross section for the production of isolated photons with transverse energies (E_T^γ) above 10 GeV and pseudorapidities $|\eta| < 2.5$ in $p\overline{p}$ collisions at $\sqrt{s} = 1.8$ TeV. The results are based on a data sample of 107.6 pb^{-1} recorded during 1992–1995 with the D0 detector

at the Fermilab Tevatron collider. The background, predominantly from jets which fragment to neutral mesons, was estimated using the longitudinal shower shape of photon candidates in the calorimeter. The measured cross section is in good agreement with the next-to-leading order QCD calculation for $E_T^\gamma \gtrsim 36$ GeV.

PACS numbers: 13.85.Qk, 12.38.Qk

Direct (or prompt) photons, by which we mean those produced in a hard parton-parton interaction, provide a probe of the hard scattering process which minimizes confusion from parton fragmentation or from experimental issues related to jet identification and energy measurement [1]. In high energy $p\overline{p}$ collisions the dominant mode for production of photons with moderate transverse energy E_T^γ is through the strong Compton process $qg \rightarrow q\gamma$. The direct photon cross section is thus sensitive to the gluon distribution in the proton. Direct-photon measurements allow tests of next-to-leading order (NLO) and resummed QCD calculations, phenomenological models of gluon radiation, and studies of photon isolation and the fragmentation process.

Data from previous collider measurements [2–4] have indicated an excess of photons at low E_T^γ ($\lesssim$25 GeV) compared with predictions of NLO QCD. This excess may originate in additional gluon radiation beyond that included in the QCD calculation [5], or reflect inadequacies in the parton distributions and fragmentation contributions [6].

In this Letter, we present a new measurement of the cross section for production of isolated photons with $E_T^\gamma \geq 10$ GeV and pseudorapidity $|\eta| < 2.5$ in $p\overline{p}$ collisions at $\sqrt{s} = 1.8$ TeV, which supersedes our previous publication [4]. (Pseudorapidity is defined as $\eta = -\ln\tan\frac{\theta}{2}$, where θ is the polar angle with respect to the proton beam.) The higher statistical precision afforded by the increased luminosity (12.9 ± 0.7 pb^{-1} recorded during 1992–1993 and 94.7 ± 5.1 pb^{-1} recorded during 1994–1995) motivated a refined estimation of the backgrounds. In particular, fully simulated jet events were used in place of single neutral mesons to model background.

Photon candidates were identified in the D0 detector [7] as isolated clusters of energy depositions in the uranium and liquid-argon sampling calorimeter. The calorimeter covered $|\eta| \lesssim 4$ and had electromagnetic (EM) energy resolution $\sigma_E/E \approx 15\%/\sqrt{E(\mathrm{GeV})} \oplus 0.3\%$. The EM section of the calorimeter was segmented longitudinally into four layers (EM1–EM4) of 2, 2, 7, and 10 radiation lengths, respectively, and transversely into cells in pseudorapidity and azimuthal angle $\Delta\eta \times \Delta\phi = 0.1 \times 0.1$ (0.05×0.05 at shower maximum in EM3). Drift chambers in front of the calorimeter were used to distinguish photons from electrons, or from photon conversions, by ionization measurement.

A three-level trigger was employed during data taking. The first level used scintillation counters near the beam pipe to detect an inelastic interaction; the second level required that the EM energy in calorimeter towers of size $\Delta\eta \times \Delta\phi = 0.2 \times 0.2$ be above a programmable threshold. The third level was a software trigger in which clusters of calorimeter cells were required to pass minimal criteria on shower shape.

Off-line, candidate clusters were accepted within the regions $|\eta| < 0.9$ (central) and $1.6 < |\eta| < 2.5$ (forward) to avoid intercalorimeter boundaries; in the central region, clusters were required to be more than 1.6 cm from azimuthal boundaries of modules. The event vertex was required to be within 50 cm of the nominal center of the detector along the beam. Each candidate was required to have a shape consistent with that of a single EM shower, to deposit more than 96% of the energy detected in the calorimeter in the EM section, and to be isolated as defined by the following requirements on the transverse energy observed in the annular region between $\mathcal{R} = \sqrt{\Delta\eta^2 + \Delta\phi^2} = 0.2$ and $\mathcal{R} = 0.4$ around the cluster: $E_T^{\mathcal{R}\leq 0.4} - E_T^{\mathcal{R}\leq 0.2} < 2$ GeV. The combined efficiency of these selections was estimated as a function of E_T^γ using a detailed Monte Carlo simulation of the detector [8] and verified with electrons from $Z \rightarrow ee$ events, and found to be 0.65 ± 0.01 (0.83 ± 0.01) at $E_T^\gamma = 40$ GeV for central (forward) photons. An uncertainty of 2.5% was added in quadrature to this to allow for a possible dependence on instantaneous luminosity. Photon candidates were rejected if there were tracks within a road $\Delta\theta \times \Delta\phi \approx 0.2 \times 0.2$ rad between the calorimeter cluster and the primary vertex. The mean efficiency of this requirement was measured to be 0.83 ± 0.01 (0.54 ± 0.03) in the central (forward) region. The inefficiency stemmed mainly from photon conversions and overlaps of photons with charged tracks (either from the underlying event or from other $p\overline{p}$ interactions).

Background to the direct-photon signal comes primarily from two-photon decays of π^0 and η mesons produced in jets. While the bulk of this background is rejected by the selection criteria (especially the isolation requirement), substantial contamination remains, predominantly from fluctuations in jet fragmentation, which can produce neutral mesons that carry most of the jet energy. For a π^0 meson with $E_T^\gamma \gtrsim 10$ GeV, the showers from its two-photon decay coalesce and mimic a single photon in the calorimeter.

The fraction of the remaining candidates that are genuine direct photons (the purity $\mathcal{P}$) was determined using the energy E_1 deposited in the first layer (EM1) of the calorimeter. The decays of neutral mesons primarily responsible for background produce two nearby photons, and the probability that at least one of them undergoes a conversion to an e^+e^- pair either in the cryostat of the calorimeter or the first absorber plate is

roughly twice that for a single photon. Such showers due to meson decays therefore start earlier in the calorimeter than showers due to single photons and yield larger E_1 depositions for any initial energy. A typical distribution in our discriminant, $\log_{10}[1 + \log_{10}\{1 + E_1(\mathrm{GeV})\}]$, is shown in Fig. 1. This variable emphasized differences between direct photons and background and was insensitive to noise and event pileup. A small correction, based on electrons from W decays, was made to bring the E_1 distribution for the 1992–1993 data into agreement with the 1994–1995 data. The distribution in the discriminant was then fitted to the sum of a photon signal and jet background, both of which were obtained from Monte Carlo simulation. Two components of the jet background were included separately: those with and those without charged tracks inside the inner isolation cone ($\mathcal{R} = 0.2$ from the photon candidate). This was done to minimize constraints in the fit from the (relatively poorly determined) tracking efficiency and from the model used for jet fragmentation.

Direct photon and QCD jet events were generated using PYTHIA [9] and then passed through the GEANT detector-simulation package, and overlaid with data acquired using a random trigger to model noise, pileup, underlying event, and multiple $p\overline{p}$ interactions [8]. The simulated E_1 was corrected for imperfect modeling of the material in the detector. We assumed that the Monte Carlo energy could be parametrized as $E_1^{\mathrm{MC}} = \alpha + \beta E_1$, with the parameters α and β determined from data: β from the $W \to e\nu$ sample and α from the photon data. The fits to extract the purity $\mathcal{P}$ were performed for different values of α, and the total χ^2 was minimized for all E_T^γ.

To reduce computation time, the jet background events were preselected just after their generation to have highly electromagnetic jets. The background subtraction technique used in this analysis employs fully simulated jet events, whereas the previous analysis modeled the background with isolated neutral mesons. With our increased statistics, it was found that individual isolated mesons could not adequately model the background. Indeed, our simulation shows that less than half of the background can be attributed to the presence of single neutral mesons within the inner isolation cones (of $\mathcal{R} = 0.2$). The new approach provided a much better description of the shower shape and isolation energy and resulted in an increased estimate of the signal purity.

Fitting was done separately for samples at central and forward regions, for each E_T^γ bin, using the package HMCMLL [10], with the constraint that the fractions of signal and background were between 0.0 and 1.0. The resulting purity $\mathcal{P}$ and its uncertainty are shown in Fig. 2 as a function of E_T^γ. As well as the fitting error, a systematic error was assigned to the use of PYTHIA to model jets. This uncertainty was estimated by varying the multiplicity of neutral mesons in the core of the jet by $\pm 10\%$ [11].

The differential cross section $d^2\sigma/dE_T^\gamma d\eta$, determined after correction for purity and efficiency (but not corrected for energy resolution) is shown as a function of E_T^γ in Fig. 3 and in Table I. The purity corrections were applied point by point, using the same binning for the cross section as for the determination of purity. The correlated errors consist of the quadrature sum of the uncertainties on luminosity, vertex requirements, and energy scale in the Monte Carlo (which are energy independent) and the model for fragmentation (large uncertainty at low E_T^γ because of the

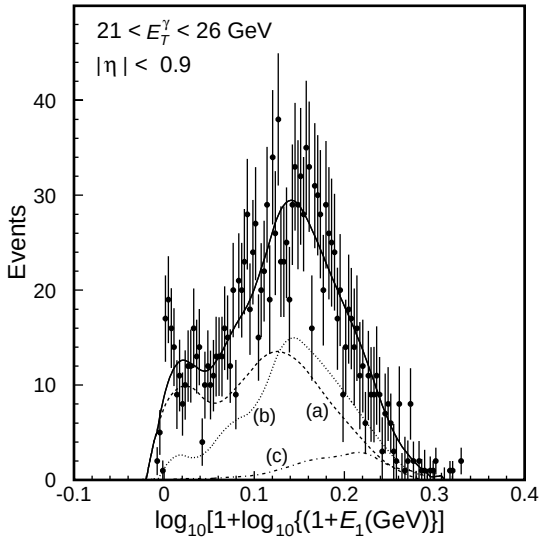

FIG. 1. Distribution of the discriminant variable for $21 < E_T^\gamma < 26$ GeV central photon candidates (points with error bars) and the fitted distribution (solid curve) composed of Monte Carlo photons [curve labeled (a)] and jets with and without charged particles [curves labeled (c) and (b), respectively]. The Monte Carlo curves shown here were smoothed for clarity (this was not done in the fitting itself). Results of these fits provide the purity $\mathcal{P}$ of the signal: for this bin, $\mathcal{P} = 0.58 \pm 0.07$.

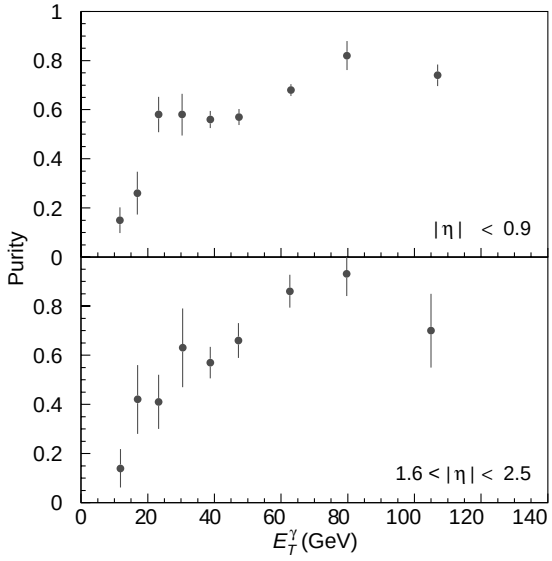

FIG. 2. The fraction of photon candidates that are direct photons as a function of E_T^γ, for central and forward photons.

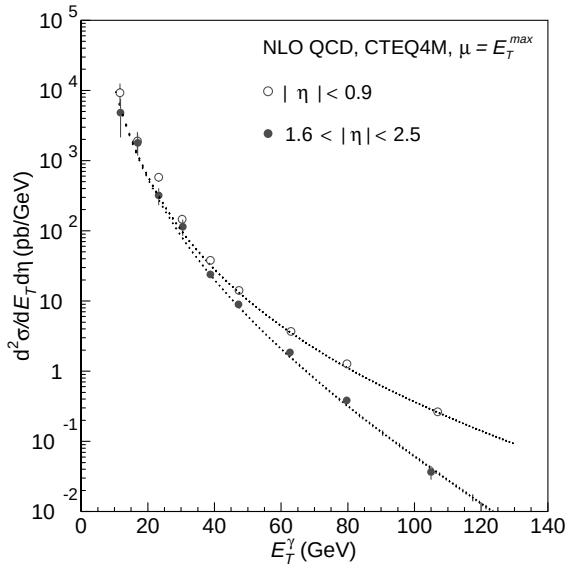

FIG. 3. The cross section $d^2\sigma/dE_T^\gamma d\eta$ for isolated photons as a function of transverse energy E_T^γ, for central and forward regions. The curves show the NLO QCD calculated cross sections.

low purity in this region). The uncorrelated errors include the statistical uncertainty, the fitting error, and the statistical uncertainties on the determination of acceptance, trigger efficiency, and the efficiency of the selection criteria.

These new measurements are $\approx(20-30)\%$ higher than our previously published results. The change is well understood and is due to the improvements in the Monte Carlo model used to estimate the purity, and in calculations of the acceptance and luminosity [12].

We compare the measured cross section with NLO QCD calculations using the program of Baer, Ohnemus, and Owens [13]. This calculation includes γ + jet, γ + two jets, and two jets with bremsstrahlung in the final state. In the latter case, a jet collinear with the photon was created with the remaining fraction of the energy of the relevant final-state parton, so that the isolation cut could be modeled. For all sources of signal, the final-state parton energies were smeared using the measured EM and jet resolutions. The isolation criterion was imposed by rejecting events with a jet of $E_T > 2$ GeV within $\mathcal{R} \leq 0.4$ of the photon. (Smearing photon and jet energies changed the QCD prediction by less than 4%.) CTEQ4M parton distributions [14] were used in the NLO calculations, with renormalization and factorization scales $\mu_R = \mu_F = E_T^{\max}$, where $E_T^{\max}$ is the larger of the transverse energies of the photon or the leading jet. If, instead, the scales $\mu_R = \mu_F = 2E_T^{\max}$ or $E_T^{\max}/2$ were employed, the predicted cross sections changed by $\lesssim 6\%$.

Figure 4 shows the difference between experimental and theoretical differential cross sections ($d^2\sigma/dE_T^\gamma d\eta$), divided by the theoretical values. In both central and forward regions, the NLO QCD predictions agree with the data for transverse energies $E_T^\gamma \gtrsim 36$ GeV. At lower transverse energies, particularly for $|\eta| < 0.9$, our measured cross section exceeds the expectation from NLO QCD, a trend consistent with previous observations at collider [2–4] and fixed target [15] energies. Using contributions from both correlated and uncorrelated errors, the χ^2 value for the data compared with NLO QCD is 8.9 in the central region and 1.9 in the forward region, for $E_T^\gamma \leq 36$ GeV in each case (the first four data points).

TABLE I. The predicted and measured cross sections in bins of E_T^γ. $\langle E_T^\gamma \rangle$ is the average photon transverse energy in each bin. The columns labeled $\delta\sigma_U$ and $\delta\sigma_C$ show the magnitude of the uncorrelated and correlated uncertainties, respectively. (The statistical error is contained in $\delta\sigma_U$.)

E_T^γ bin (GeV)	$\langle E_T^\gamma \rangle$ (GeV)	$d^2\sigma/dE_T^\gamma d\eta$ (pb/GeV) NLO QCD	measured	$\delta\sigma_U$ (%)	$\delta\sigma_C$ (%)
		$\lvert\eta\rvert < 0.9$			
10.0–14.0	11.7	6030	9270	35	74
14.0–21.0	16.9	1250	1910	34	27
21.0–26.0	23.3	310	579	13	17
26.0–36.0	30.3	97.9	146	15	14
36.0–42.0	38.8	32.5	37.8	7.1	13
42.0–54.0	47.4	13.1	14.1	6.7	12
54.0–75.0	63.0	3.52	3.69	4.8	11
75.0–85.0	79.8	1.12	1.28	8.3	11
85.0–140.0	106.8	0.258	0.264	7.1	10
		$1.6 < \lvert\eta\rvert < 2.5$			
10.0–14.0	11.8	5760	4850	56	34
14.0–21.0	17.0	1160	1780	34	26
21.0–26.0	23.3	279	318	27	20
26.0–36.0	30.5	77.9	115	26	17
36.0–42.0	38.8	23.6	23.8	12	14
42.0–54.0	47.2	8.36	8.97	11	12
54.0–75.0	62.6	1.61	1.85	8.3	11
75.0–85.0	79.7	0.327	0.384	11	10
85.0–140.0	105.1	0.0414	0.0366	23	10

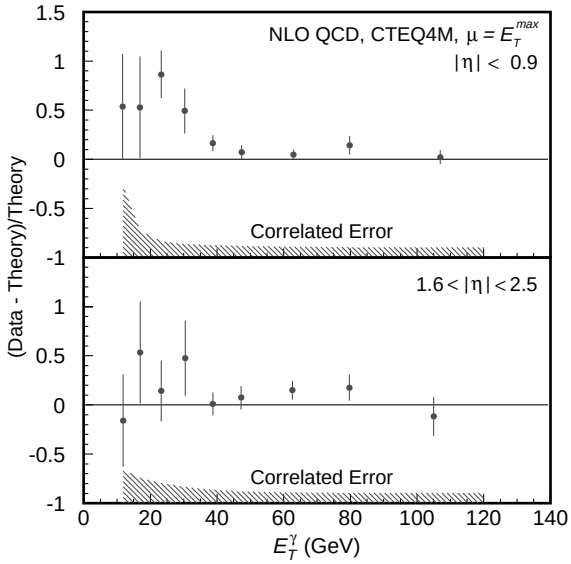

FIG. 4. Difference between the measured differential cross section for isolated photon production and the prediction from NLO QCD, using CTEQ4M parton distributions.

These data complement and extend previous measurements and provide additional input for extraction of parton distributions through global fits to all data. The difference between the data and NLO QCD for $E_T^\gamma \lesssim 36$ GeV suggests that a more complete theoretical understanding of processes that contribute to the low-E_T^γ behavior of the photon cross section is needed.

We thank J. F. Owens for his assistance with the theoretical calculations. We thank the Fermilab and collaborating institution staffs for contributions to this work, and we acknowledge support from the Department of Energy and National Science Foundation (USA), Commissariat à L'Energie Atomique (France), Ministry for Science and Technology and Ministry for Atomic Energy (Russia), CAPES and CNPq (Brazil), Departments of Atomic Energy and Science and Education (India), Colciencias (Colombia), CONACyT (Mexico), Ministry of Education and KOSEF (Korea), CONICET and UBACyT (Argentina), A. P. Sloan Foundation, and the Humboldt Foundation.

[1] G. R. Farrar, Phys. Lett. **67B**, 337 (1977).
[2] UA2 Collaboration, J. Alitti *et al.,* Phys. Lett. B **263**, 544 (1991).
[3] CDF Collaboration, F. Abe *et al.,* Phys. Rev. D **48**, 2998 (1993); Phys. Rev. Lett. **73**, 2662 (1994).
[4] D0 Collaboration, S. Abachi *et al.,* Phys. Rev. Lett. **77**, 5011 (1996).
[5] J. Huston *et al.,* Phys. Rev. D **51**, 6139 (1995); H.-L. Lai and H.-N. Li, Phys. Rev. D **58**, 114020 (1998); L. Apanasevich *et al.,* Phys. Rev. D **59**, 074007 (1999).
[6] M. Glück, L. E. Gordon, E. Reya, and W. Vogelsang, Phys. Rev. Lett. **73**, 388 (1994); W. Vogelsang and A. Vogt, Nucl. Phys. **B453**, 334 (1995).
[7] D0 Collaboration, S. Abachi *et al.,* Nucl. Instrum. Methods Phys. Res., Sect. A **338**, 185 (1994).
[8] J. Womersley, in *Proceedings of the 26th International Conference on High Energy Physics, Dallas, TX, 1992* (Fermilab Report No. Fermilab-Conf-92-306, 1992).
[9] T. Sjöstrand, Comput. Phys. Commun. **82**, 74 (1994). Version 5.7 was used in this analysis.
[10] R. Barlow and C. Beeston, Comput. Phys. Commun. **77**, 219 (1993).
[11] Suggested as an estimate of uncertainty in the neutral meson multiplicity, based on comparisons with LEP data [T. Sjöstrand (private communication)].
[12] J. Bantly *et al.,* Fermilab Report No. Fermilab-TM-1930, 1996 (unpublished). In order to facilitate comparison with earlier data, this analysis does not use the luminosity normalization given in D0 Collaboration, B. Abbott *et al.,* hep-ex/990625, Sec. VII, pp. 21–22, Phys. Rev. D (to be published). The updated normalization would have the effect of increasing the luminosity by 3.2%.
[13] H. Baer, J. Ohnemus, and J. F. Owens, Phys. Rev. D **42**, 61 (1990).
[14] CTEQ Collaboration, H. L. Lai *et al.,* Phys. Rev. D **55**, 1280 (1997).
[15] E706 Collaboration, L. Apanasevich *et al.,* Phys. Rev. Lett. **81**, 2642 (1998).